Preliminary Amplitude Analysis of the $D^0 \to K^+K^-\pi^0$ decay at LHCb

Pio Francesco Varrella
Reviewers: Dr. Federico Betti, Prof. Angelo Carbone

TUDo, UniBo & UCA

LHCb experiment and INFN Bologna

September 29, 2025

Outline

Outline

CP Symmetry

- The *CP* Violation does not explain the matter-antimatter unbalance
- Resonant decays provide a new realm for *CPV* searches:
  - more information to be extracted
  - indirect searches of New Physics
- *CPV* observed in strange, beauty and charm mesons and recently in beauty baryons
- *CPV* not yet observed in charmed baryons

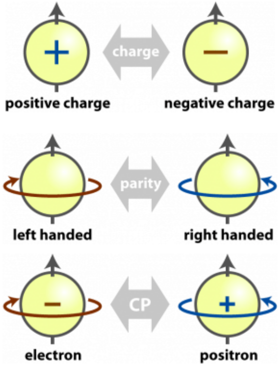

Why $D^0 \to K^+K^-\pi^0$?

- Presence of intermediate resonances
- Characterization of the $K\pi$ system scalar part at lower energies
- Probe for New Physics beyond the Standard Model:
  - higher sensitivity to *CPV* along the phase space
  - Single Cabibbo-suppressed decay with penguin-level diagrams contributing to the full amplitude

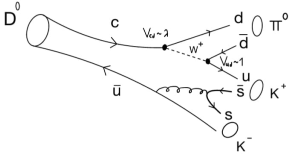

(a) Tree-level Feynman diagram

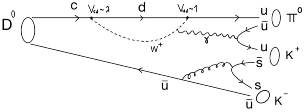

(b) Penguin-level Feynman diagram

Analysis state-of-the-art

- Amplitude analysis (or Dalitz analysis): a tool to understand the resonances contributions and their interferences
- Only one $D^0 \to K^+K^-\pi^0$ Dalitz analysis in literature coming from the BaBar experiment [https://journals.aps.org/prd/abstract/10.1103/PhysRevD.76.011102]
- **First attempt of a $D^0 \to K^+K^-\pi^0$ Dalitz analysis within the LHCb experiment**
    - BaBar plots:

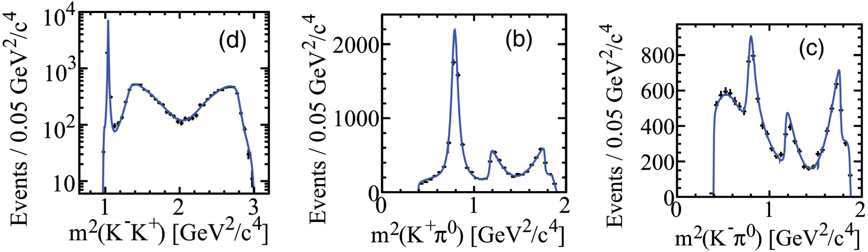

Outline

The LHCb experiment

- One of the experiments of the LHC @CERN
- Objective: phenomenology of b and c hadrons and CPV parameters
- The LHCb detector: single-arm forward spectrometer
- Large $c\bar{c}$ production cross section: $\sim 2.8\,\text{mb}$ at @ $13\,\text{TeV}$ ($\sim 10^6$ pairs per second)

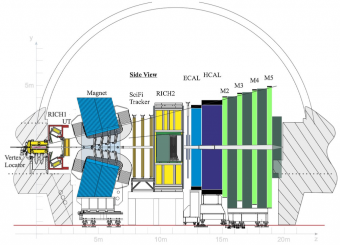

LHCb experiment: data of the analysis

- *pp* interactions at $\sqrt{s} = 13$ TeV (Run 2) and $\sqrt{s} = 13.6$ TeV (Run 3)
- 2016-2018 samples (Run 2) and 2024 sample (Run 3)
- 5.4 fb^{-1} (Run 2) and 7.2 fb^{-1} (2024) of good-for-physics recorded data
- Around 8 fb^{-1} of data recorded so far in 2025

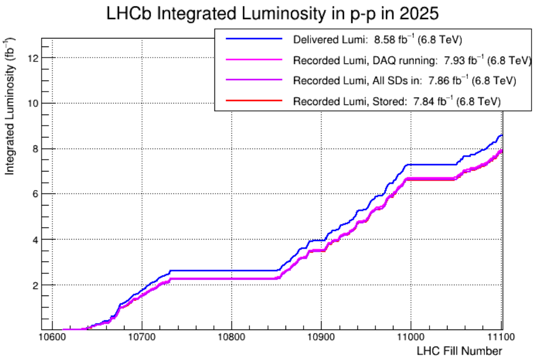

Outline

$D^0 \to K^+ K^- \pi^0$ decay channel

- Prompt $D^{*+} \to D^0(\to K^+ K^- \pi^0)\pi^+_{soft}$ decays
- Production flavour of the D^0 is determined from the soft (low-P) pion charge
- π^0 reconstructed from ECAL cells $\to$ two different topologies:
  - Resolved
  - Merged

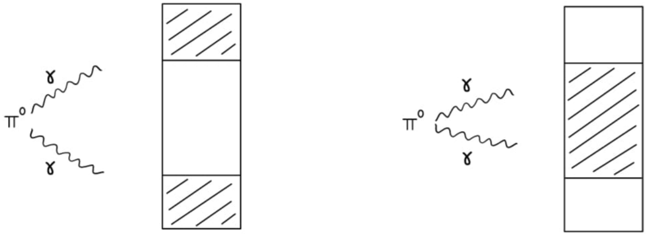

Comparison between Resolved Run 2 and Run 3 samples

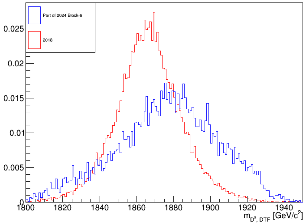

Figure 2: $m_{D^0,DTF}$

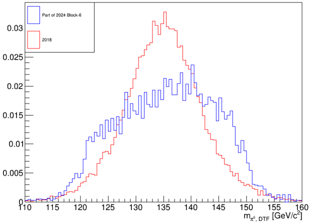

Figure 3: $m_{\pi^0,DTF}$

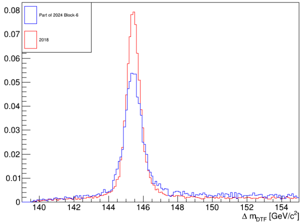

Figure 4: Δm_{DTF}

- 2018 sample from Run 2 and 2024 sample from Run 3
- DecayTreeFitter to re-evaluate the decay topology by requiring the D^{*+} comes from primary pp collisions
- Low Q-value: $Q \equiv m_{D^{*+}} - m_{D^0} - m_{\pi_{soft}}$

Discriminant fit to Δm_{DTF}

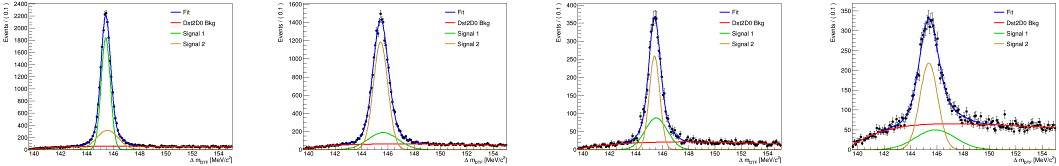

(a) Resolved 2018 (b) Merged 2018 (c) Resolved 2024 (d) Merged 2024

- Multicomponent fit model:
  - Signal: Gaussian + Gaussian
  - Background: Dst2D0Bg

Extrapolated yields and purities

	N_S^{extr}	**Purity**	$N_S^{extr} / \mathcal{L}_{int}$ (pb)
Res 2018	110 250	90.71%	20.14
Mer 2018	102 896	89.21%	19.05
Res 2024	304 560	82.25%	43.88
Mer 2024	360 122	82.23%	51.89

- Yields per lumi block higher in 2024 but greater purity in 2018

- SPlot technique: assignment of **sWeights** to every event in the sample
- Applying the sWeights signal and background distributions can be statistically separated

Dalitz projections of the Resolved 2018 sample

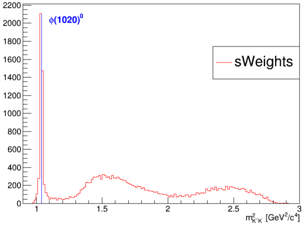

Figure 6: $m^2_{K^+K^-}$

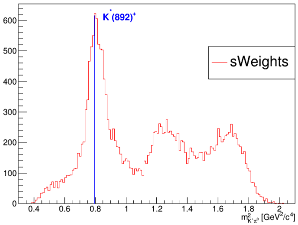

Figure 7: $m^2_{K^+\pi^0}$

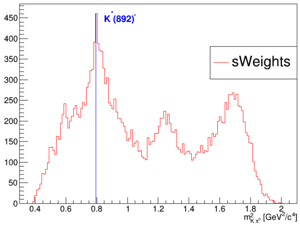

Figure 8: $m^2_{K^-\pi^0}$

- $\phi(1020)^0, K^*(892)^{\pm}$ resonances are the major visible contributions

Dalitz plots of the Resolved 2018 sample

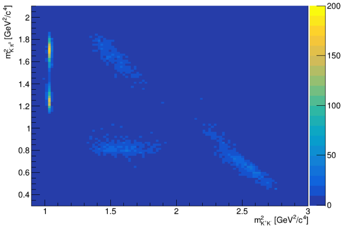

Figure 9: $m^2_{K^-\pi^0}$ vs $m^2_{K^+K^-}$

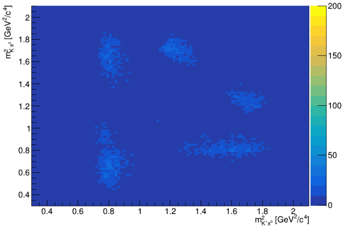

Figure 10: $m^2_{K^-\pi^0}$ vs $m^2_{K^+\pi^0}$

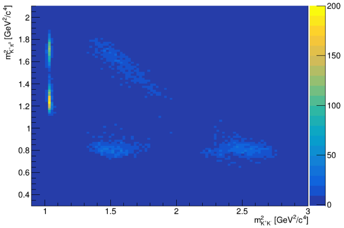

Figure 11: $m^2_{K^+\pi^0}$ vs $m^2_{K^+K^-}$

- Resonances associated with two of the planes manifest as vertical or horizontal structures, while those from the third plane appear diagonally
- 2-lobes structures $\longrightarrow$ vectorial (spin-1) resonances

Amplitude fit

$$\underbrace{\mathcal{A}}_{\textit{total amplitude}} = \sum_r \underbrace{c_r}_{\text{complex coefficient}} \underbrace{A_r}_{\text{intermediate amplitude}} \qquad A_r :\ D^0 \to a\, r\, (\to b\, c)$$

- c_r are found by minimising (within the AmpGen framework):

$$-2 ln\, \mathcal{L} = -2 \sum_i ln\, \overbrace{P(x_i; c)}^{\textit{total PDF}} \qquad -2 ln\, \mathcal{L} = -2 \frac{\sum_i \overbrace{sw_i}^{\textit{sWeight}}}{\sum_i sw_i^2} \sum_i sw_i\, ln\, \overbrace{P_s(x_i; c)}^{\textit{signal PDF}}$$

- $P_s(x; c) = \frac{\epsilon(x) S(x;c) \Phi_3(x)}{I(c)}$ with $S(x; c) = |\mathcal{A}|^2$, $\epsilon(x)$ acceptance and efficiency over the PHSP, $\Phi_3(x)$ density of the PHSP
- $I(c) = \int \epsilon(x) S(x; c) \Phi_3(x)\, d^2x \simeq \frac{I^{gen}}{N_{MC}} \sum_{i=0}^{N_{MC}} \frac{S(x;c)}{S^{gen}(x)} \qquad [I^{gen} = \int \epsilon(x) S^{gen}(x) \Phi_3(x) d^2x]$

Fit and interference fractions

- c_r are convention-dependent $\longrightarrow$ no direct comparison
- Convention-independent objects to quantify the amplitudes contributions:
  - Fit Fraction (FF_i): $\frac{\int |c_i A_i(x)|^2 d^2x}{\int |\sum_j c_j A_j(x)|^2 d^2x}$
  - Interference Fraction (FF_{ij}): $\frac{\int 2Re\left[c_i c_j A_i(x) A_j^*(x)\right] d^2x}{\int |\sum_k c_k A_k(x)|^2 d^2x}$
- Interferences between amplitudes can show up $\longrightarrow \sum_i FF_i \neq 1$

Amplitude model

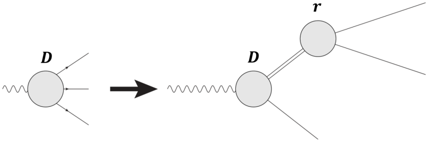

- **Isobar** formalism is adopted
- Coherent Sum of intermediate amplitudes seen the pseudo-scalar nature of the decay

$$\mathcal{A}(m_{ab}^2, m_{bc}^2) = \sum_r c_r \mathcal{A}_r(m_{ab}^2, m_{bc}^2)$$

$$\mathcal{A}_r(m_{ab}^2, m_{bc}^2) = \underbrace{F_D^{(L)}(q, q_0)}_{\text{Blatt-Weisskopf form factor}} \underbrace{Z_L(m_{ab}^2, m_{bc}^2)}_{\text{Resonance spin factor}} \underbrace{\tau_r(m_{bc})}_{\text{Resonance lineshape}} \underbrace{F_r^{(L)}(p, p_0)}_{\text{Blatt-Weisskopf form factor}}$$

Monte Carlo simulation strategy

- A full LHCb $D^0 \to K^+K^-\pi^0$ simulation sample is missing

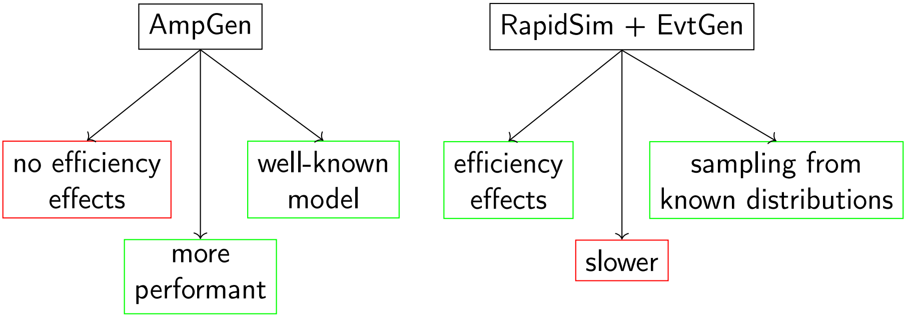

- VSS model for $D^{*+} \to D^0\pi^+_{soft}$, BaBar-based model for $D^0 \to K^+K^-\pi^0$
- Momentum smearing derived from the full $D^{*+} \to D^0(\to \pi^+\pi^-\pi^0)\pi^+_{soft}$ simulation sample

Kinematics of the produced RapidSim+EvtGen sample

■ sWeights ■ RapidSim

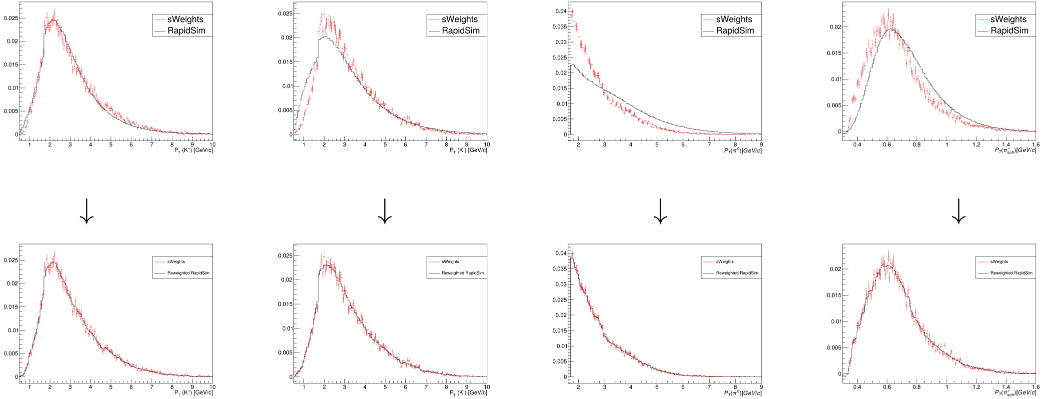

- Gradient Boosted Reweighter method (used variables: P_T, η, ϕ of $K^{\pm}, \pi^0$ and P_T of π^+_{soft})

■ sWeights ■ RapidSim

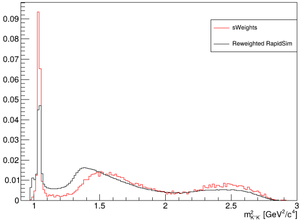

Figure 12: $m^2_{K^+K^-}$

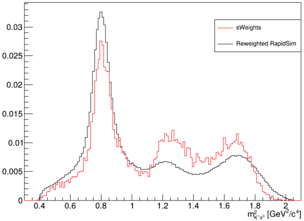

Figure 13: $m^2_{K^+\pi^0}$

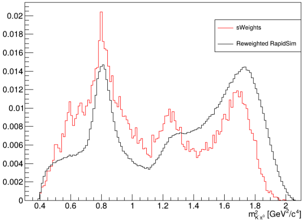

Figure 14: $m^2_{K^-\pi^0}$

Validation of the AmpGen fitter

- $D^0 \to \pi^+\pi^-\pi^0$ as validation channel
- Full simulation sample is present

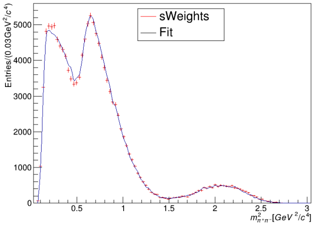

Figure 15: $m^2_{\pi^+\pi^-}$

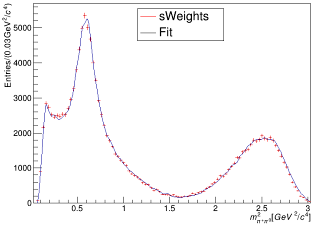

Figure 16: $m^2_{\pi^+\pi^0}$

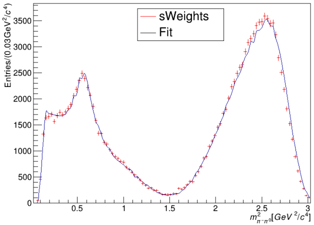

Figure 17: $m^2_{\pi^-\pi^0}$

Validation of the AmpGen Fitter [2]

Resonance	Our FF_i [%]	Reference FF_i [%]	Fixed/Free c_r
$\rho(770)^+$	65.98 $\pm$ 1.03	75.07 $\pm$ 0.07	fixed
$\rho(770)^0$	40.58 $\pm$ 0.68	32.89 $\pm$ 0.05	free
$\rho(770)^-$	29.39 $\pm$ 0.26	26.52 $\pm$ 0.06	free
$\rho(1450)^+$	0.48 $\pm$ 0.41	0.72 $\pm$ 0.01	free
$\rho(1450)^0$	0.190 $\pm$ 0.003	0.03 $\pm$ 0.01	fixed
$\rho(1450)^-$	0.215 $\pm$ 0.003	0.03 $\pm$ 0.01	fixed
$\rho(1700)^+$	0.87 $\pm$ 0.34	0.26 $\pm$ 0.02	free
$\rho(1700)^0$	1.19 $\pm$ 0.04	0.10 $\pm$ 0.01	free
$\rho(1700)^-$	0.085 $\pm$ 0.046	0.07 $\pm$ 0.01	free
$f_2(1270)^0$	1.15 $\pm$ 0.04	0.59 $\pm$ 0.01	free
$\pi\pi$ S-wave (k-Matrix)	2.36 $\pm$ 0.04	1.55 $\pm$ 0.01	free

- Observable mismatches are not due to the AmpGen fit $\longrightarrow$ AmpGen fitter works well

Fit to $K^+K^-\pi^0$ sWeights with the reweighted RapidSim+EvtGen sample

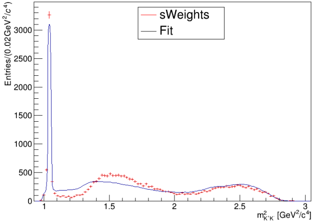

Figure 18: $m^2_{K^+K^-}$

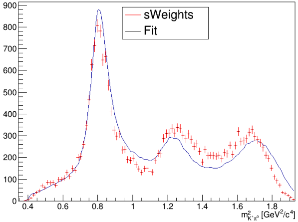

Figure 19: $m^2_{K^+\pi^0}$

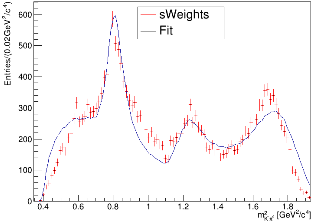

Figure 20: $m^2_{K^-\pi^0}$

- No visual agreement
- Problem with the relative contributions of the resonances

Fit to $K^+K^-\pi^0$ sWeights: fit fractions

Resonance	Our FF_i [%]	BaBar FF_i [%]
$K^*(892)^+$	2.7 ± 0.3	$45.2 \pm 0.8 \pm 0.6$
$K^*(1410)^+$	13.4 ± 1.1	$3.7 \pm 1.1 \pm 1.1$
$K^+\pi^0(S)$	35.1 ± 2.2	$16.3 \pm 3.4 \pm 2.1$
$\phi(1020)^0$	5.6 ± 0.3	$19.3 \pm 0.6 \pm 0.4$
$f_0(980)$	34.4 ± 2.4	$6.7 \pm 1.4 \pm 1.2$
$f_2'(1525)$	0.70 ± 0.10	$0.08 \pm 0.04 \pm 0.05$
$K^*(892)^-$	0.88 ± 0.13	$16.0 \pm 0.8 \pm 0.6$
$K^*(1410)^-$	23.0 ± 1.1	$4.8 \pm 1.8 \pm 1.2$
$K^-\pi^0(S)$	95.0 ± 4.3	$2.7 \pm 1.4 \pm 0.8$
$\sum_i FF_i$	211 ± 7	$115 \pm 11 \pm 8$

- Different conventions and normalisation among AmpGen, EvtGen and the BaBar experiment
- Difficulty to map the BaBar values of the coefficients in AmpGen

AmpGen-in-RapidSim alternative strategy

- Sample generated in AmpGen according to the discussed model
  - Iterative procedure to find a valid set of coefficient values almost reproducing the BaBar case
- The produced kinematics of D^0-daughters is used as input for a new signal sample generated in RapidSim
- The obtained data-simulation sample agreement is not optimal but at least improved with respect to the previous case

Comparison of AmpGen-in-RapidSim sample with reweighted RapidSim+EvtGen sample

- sWeights
- RapidSim

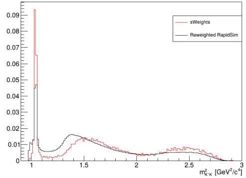

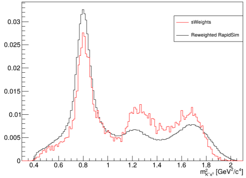

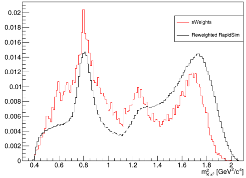

↓ ↓ ↓

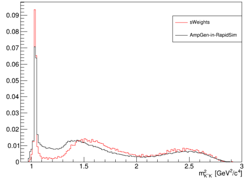

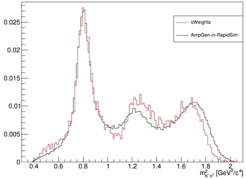

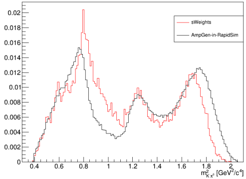

AmpGen-in-RapidSim strategy: fit result

- Visually unsatisfactory

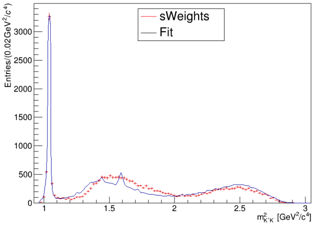

Figure 21: $m^2_{K^+K^-}$

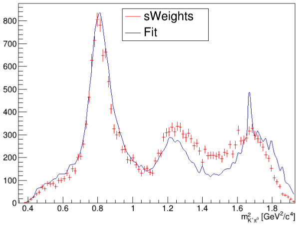

Figure 22: $m^2_{K^+\pi^0}$

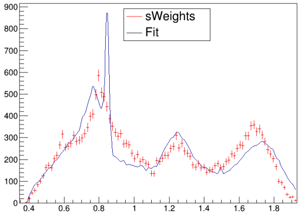

Figure 23: $m^2_{K^-\pi^0}$

AmpGen-in-RapidSim strategy: fit fractions

Resonance	Our FF_i [%]]	BaBar FF_i [%]
$K^*(892)^+$	34.6 ± 0.5	$45.2 \pm 0.8 \pm 0.6$
$K^*(1410)^+$	7.1 ± 0.7	$3.7 \pm 1.1 \pm 1.1$
$K^+\pi^0(S)$	101 ± 6	$16.3 \pm 3.4 \pm 2.1$
$\phi(1020)^0$	23.3 ± 0.3	$19.3 \pm 0.6 \pm 0.4$
$f_0(980)$	26.9 ± 2.4	$6.7 \pm 1.4 \pm 1.2$
$f_2'(1525)$	0.012 ± 0.012	$0.08 \pm 0.04 \pm 0.05$
$K^*(892)^-$	40.2 ± 0.8	$16.0 \pm 0.8 \pm 0.6$
$K^*(1410)^-$	5.1 ± 0.5	$4.8 \pm 1.8 \pm 1.2$
$K^-\pi^0(S)$	20.1 ± 2.9	$2.7 \pm 1.4 \pm 0.8$
$\sum_i FF_i$	259 ± 6	$115 \pm 11 \pm 8$

- Still discrepancy with BaBar fit fractions
- Temporarily not possible to reproduce the BaBar result (model) in AmpGen

Conclusion and future perspectives

- Presented preliminary results are not good due to:
  - missing full $D^* \to D^0(\to K^+ K^- \pi^0)\pi^+_{soft}$ simulation sample
  - approximate procedures used
- Reliable approach and starting model necessary for the amplitude fit
- Request a full simulation sample within the collaboration
- Get the BaBar sample to be fitted in AmpGen for the determination of the amplitudes complex coefficients
- In the meantime:
  - Investigation of the underlying relation between the AmpGen and BaBar normalisations
  - Refinement of the offline selection on data

Thanks for your attention!

Backup

Backup: Hlt1 line requirements

$$\chi^2_{IP} > 7.4\,(P_T > 25.0\,\text{GeV}/c)$$

$$ln(\chi^2_{IP}) > ln(7.4) + \frac{1.0}{(P_T - 1.0)^2} + \lambda\left(1 - \frac{P_T}{25.0}\right)\,(P_T \in [1.0, 25.0]\,\text{GeV}/c)$$

$$[P_T] = \text{GeV}/c$$

Backup: Stripping line requirements

Particle	Quantity	Selection criteria
Global Selection	Number of long tracks	< 180
$K^{\pm}$	PIDK P_T	> 7 > 0.5 GeV$/c$
K^+ or K^-	P_T	> 1.7 GeV$/c$
$K^{\pm}$ pair	m_{KK}	< 1.9 GeV$/c^2$
π^0	P_T	> 0.500 GeV$/c$
D^0	P_T $\lvert m_{K^+K^-\pi^0} - 1.86484\ \text{GeV}/c^2\rvert$ $\lvert m_{D^0} - 1.86484\ \text{GeV}/c^2\rvert$	> 1.4 GeV$/c$ < 0.160 GeV$/c^2$ < 0.150 GeV$/c^2$
π_{soft}	P_T	> 0.300 GeV$/c$
D^{*+}	$m_{D^*} - m_{D^0}$ $m_{K^+K^-\pi^0\pi_{\text{soft}}} - m_{K^+K^-\pi^0}$	< 0.180 GeV$/c^2$ < 0.185 GeV$/c^2$

Backup: Hlt2 line + offline selection requirements

Particle	Quantity	Selection criteria
$K^{\pm}$	PIDK χ^2_{IP} $\theta_{K\pi_{soft}}$	> 15 > 20 > 0.001
$K^{\pm}$ pair	m_{KK} P_T $\theta_{K^+K^-}$	< 1.9 GeV$/c^2$ > 1.9 GeV$/c$ > 0.001
π^0	P_T m_{π^0}	> 1.7 GeV$/c$ $\in [0.107, 0.163]$ GeV$/c^2$
D^0	P_T $m_{K^+K^-\pi^0}$ m_{D^0} $arcos(\mathrm{DIRA})$	> 6.0 GeV$/c$ $\in [1.700, 2.020]$ GeV$/c^2$ $\in [1.80884, 1.92884]$ GeV$/c^2$ < 0.05 rad
D^{*+}	$m_{D^{*+}} - m_{D^0}$ $m_{D^{*+},DTF} - m_{D^0,DTF}$ $m_{D^{*+}} - m_{D^0} - m_{\pi_{\mathbf{soft}}}$ $m_{K^+K^-\pi^0\pi_{\mathbf{soft}}} - m_{K^+K^-\pi^0} - m_{\pi_{\mathbf{soft}}}$ $log(\chi^2)$	> 0.1 GeV$/c^2$ $\in [0.1396, 0.155]$ GeV$/c^2$ $\in [-0.999, 0.04545]$ GeV$/c^2$ $\in [-0.185, 0.05543]$ GeV$/c^2$ < 2.3

Backup: Implemented amplitude model

- S-Wave states:
  - K^+K^-: $f_0(980)^0$ (Flatte)
  - $K^+\pi^0$: $K_0^*(1430)^+$ (LASS)
  - $K^-\pi^0$: $K_0^*(1430)^-$ (LASS)
- P-Wave states:
  - K^+K^-: $\phi(1020)^*$ (RBW)
  - $K^+\pi^0$: $K^*(892)^+, K^*(1410)^+$ (RBW)
  - $K^-\pi^0$: $K^*(892)^-, K^*(1410)^-$ (RBW)
- D-Wave states:
  - K^+K^-: $f_2'(1525)$ (RBW)

Backup: Resonance lineshape

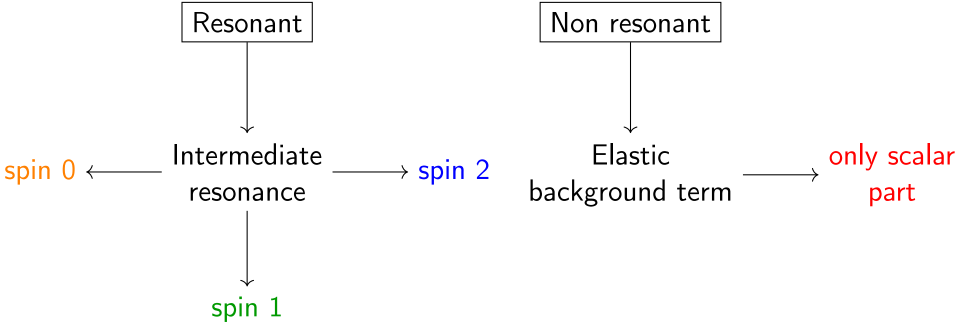

- P and D-waves: $\phi(1020)^0$, $K^*(892)^\pm$, $K^*(1410)^\pm$, $f_2(1525)$ $\longrightarrow$ RBW
- S-waves: $K_0^*(1430)^\pm$ $(K^\pm\pi^0)$, $f_0(980)$ (K^+K^-) $\longrightarrow$ LASS $(K^\pm\pi^0)$ and Flatté (K^+K^-)

Backup: RBW, LASS and Flatté shapes

- RBW: resonance with a dominant decay channel

$$\mathcal{A}_{BW}(s) = \frac{1}{(m_0^2 - s) - i m_0 \Gamma(m)}$$

- LASS: $K\pi$ S-wave system with both resonant and non-resonant terms

$$\mathcal{A}_{K\pi(S)}(s) = \underbrace{A_{NR}(s)}_{Non\ Resonant} + \underbrace{c}_{complex\ phase} \cdot \underbrace{A_R(s)}_{Resonant(RBW)}$$

- Flatté: KK S-wave system for a resonance with coupled channels $(\pi\pi, K\bar{K})$

$$\mathcal{A}_{Flatt}(s) = \frac{1}{m_0^2 - s - i m_0 (g_{\pi\pi}\rho_{\pi\pi}(s) + g_{KK}\rho_{KK}(s))}$$

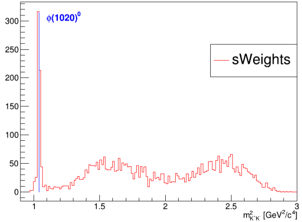

(a) $m^2_{K^+K^-}$

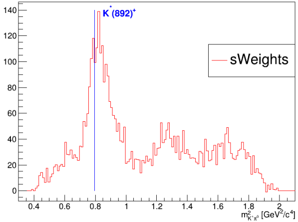

(b) $m^2_{K^+\pi^0}$

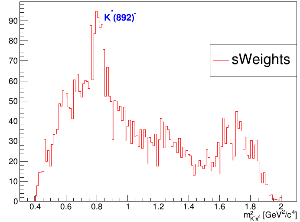

(c) $m^2_{K^-\pi^0}$

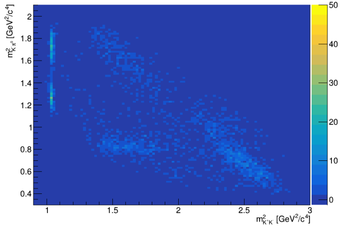

(a) $m^2_{K^-\pi^0}$ vs $m^2_{K^+K^-}$

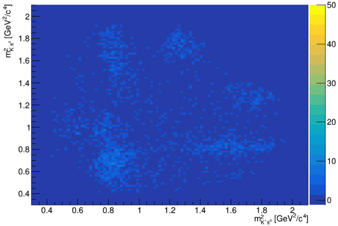

(b) $m^2_{K^-\pi^0}$ vs $m^2_{K^+\pi^0}$

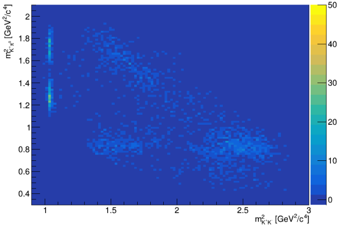

(c) $m^2_{K^+\pi^0}$ vs $m^2_{K^+K^-}$

Backup: Integration technique [1]

$$P_s(x;c) = \frac{\epsilon(x)S(x;c)\Phi_3(x)}{I(c)} = \frac{\epsilon(x)S(x;c)\Phi_3(x)}{\int \epsilon(x)S(x;c)\Phi_3(x)d^2x}$$

$$P^{\text{gen}}(x;c) = \frac{\epsilon(x)S^{\text{gen}}(x)\Phi_3(x)}{I^{\text{gen}}} = \frac{\epsilon(x)S^{\text{gen}}(x)\Phi_3(x)}{\int \epsilon(x)S^{gen}(x)\Phi_3(x)d^2x}$$

$$-\log\mathcal{L} = -\log(\prod_{j \in events} P_j(x_j;c)) = -\sum_{j \in events} \log(P_j(x_j;c))$$

$$-\log\mathcal{L} = -\sum_{j \in events} \log(\sum_{i \in pdf\ comp} P_{ji}(x_j;c)) = -\sum_{j \in events} \log(P_s(x_j;c))$$

$$-\log\mathcal{L} = \sum_{j \in \text{events}} [-\log S(x_j;c) - \log(\epsilon(x_j)\Phi_3(x_j)) + \log I(c)]$$

$$-\log\mathcal{L} = \sum_{j \in \text{events}} [-\log S(x_j;c) + \log I(c)]$$

Backup: Integration technique [2]

$$I(c) = \int \epsilon(x) S(x;c) \Phi_3(x) d^2x = \int \frac{\epsilon(x) S(x;c) \Phi_3(x)}{P^{gen}} P^{gen} d^2x$$

$$I(c) = I^{gen} \int \frac{\epsilon(x) S(x;c) \Phi_3(x)}{\epsilon(x) S^{gen}(x) \Phi_3(x)} P^{gen} d^2x = I^{gen} \int \frac{S(x;c)}{S^{gen}(x)} P^{gen} d^2x$$

$$I(c) = I^{gen} \mathbb{E}_{P^{gen}} \left[\frac{S(x;c)}{S^{gen}(x)} \right] = I^{gen} \frac{1}{N_{MC}} \sum_{i=1}^{N_{MC}} \frac{S(x;c)}{S^{gen}(x)}$$

$$-\log \mathcal{L} = \sum_{j \in \text{events}} \left[-\log S(x_j;c) + \log \left(\frac{1}{N_{MC}} \sum_{i=1}^{N_{MC}} \frac{S(x;c)}{S^{gen}(x)} \right) \right]$$

Backup: Iterative procedure [1]

- The difference is just in the scale of the couplings

$$A^2 = |c_1 A_1 + c_2 A_2 + \dots + c_n A_n|^2 = |a_1 e^{i\phi_1} A_1 + a_2 e^{i\phi_2} A_2 + \dots + a_n e^{i\phi_n} A_n|^2$$
$$= |1 \cdot e^{i \cdot 0} A_1 + a'_2 e^{i\phi'_2} A_2 + \dots + a'_n e^{i\phi'_n} A_n|^2$$

- The phase differences respect the phase of the fixed resonance are the same $\rightarrow$ same relative phases as BaBar;
- Need a way to provide every term with the right relative strength (FF_i)

Backup: Iterative procedure [2]

1. Initial setting:
   - ϕ_r fixed to the BaBar values
   - a_r set to the $\sqrt{FF_r}$
2. Generation of a MC sample;
3. Fit to the latter with one resonance ($K^*(892)^+$) and all phases fixed;
4. Upgrade a_r as:

$$a_r \leftarrow a_r \sqrt{\frac{FF_r^{exp}}{FF_r^{meas}}}$$

5. Repeat steps 2-3 till getting the BaBar fit fractions.

Backup: Iterative procedure [3]

$$FF_r = \frac{\int |a_r e^{i\phi_r} A_r|^2 d\tau}{\int |\sum_r a_r e^{i\phi_r} A_r|^2 d\tau}$$

In a sense it's like:

$$FF_r \sim a_r^2$$

that's why we start with:

$$a_r = \sqrt{FF_r^{BaBar}}$$

and then upload it with:

$$a_r \sqrt{\frac{FF_r^{BaBar}}{FF_r^{meas}}}$$

Backup: Iterative procedure [4]

- Iterative procedure following the mentioned strategy
- In every step fit fractions are compared to BaBar values, if their difference is lower than 1% in modulus the script is stopped
- In the case of fit fractions not matching perfectly, the ones closer have been retained
  - Evaluation for every step of a cost function: $\sum_r |FF_r^{BaBar} - FF_r^{meas}|$
  - In the next step the amplitude magnitudes (a_r) are upgraded only if the cost function is lower than the previous step
- $\rightarrow$ after 2 rounds the script stops

Backup: Iterative procedure [5]

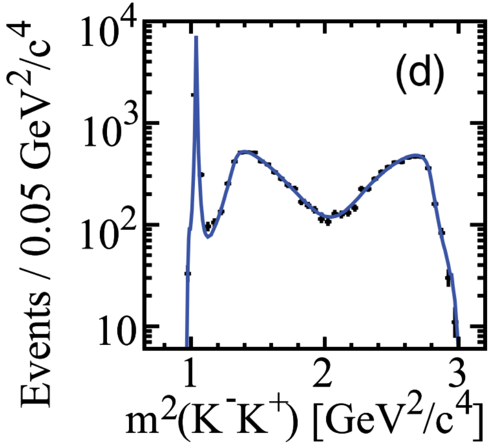

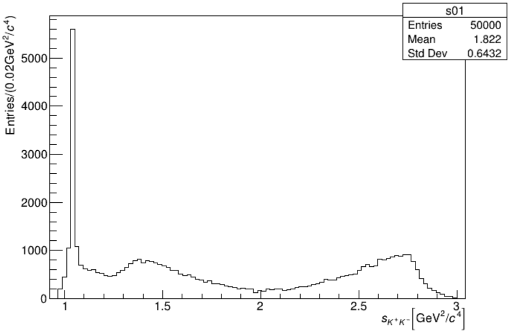

Backup: Iterative procedure [6]

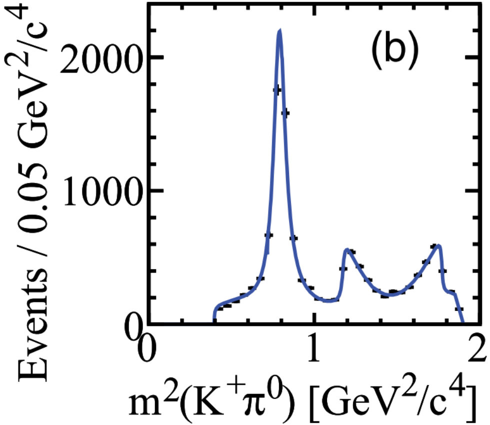

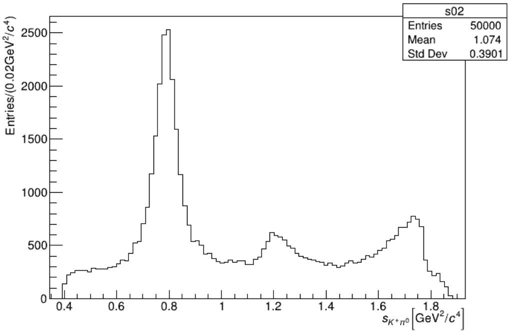

Backup: Iterative procedure [7]

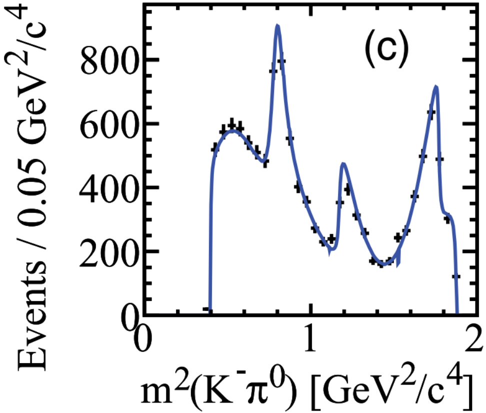

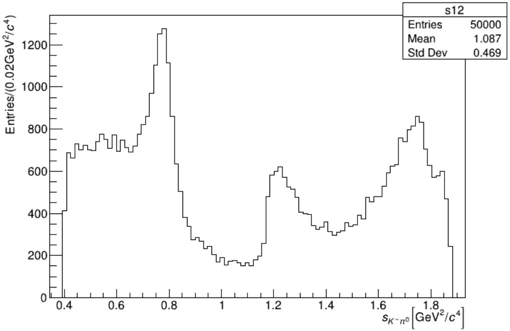

Backup: Iterative procedure [8]

Resonance	Our FF_i [%]]	BaBar FF_i [%]
$K^*(892)^+$	37.5 $\pm$ 0.3	45.2 $\pm$ 0.8 $\pm$ 0.6
$K^*(1410)^+$	1.45 $\pm$ 0.16	3.7 $\pm$ 1.1 $\pm$ 1.1
$K^+\pi^0(S)$	12.9 $\pm$ 0.7	16.3 $\pm$ 3.4 $\pm$ 2.1
$\phi(1020)^0$	13.5 $\pm$ 0.2	19.3 $\pm$ 0.6 $\pm$ 0.4
$f_0(980)$	4.9 $\pm$ 0.4	6.7 $\pm$ 1.4 $\pm$ 1.2
$f_2'(1525)$	0.08 $\pm$ 0.02	0.08 $\pm$ 0.04 $\pm$ 0.05
$K^*(892)^-$	13.0 $\pm$ 0.2	16.0 $\pm$ 0.8 $\pm$ 0.6
$K^*(1410)^-$	4.1 $\pm$ 0.15	4.8 $\pm$ 1.8 $\pm$ 1.2
$K^-\pi^0(S)$	1.9 $\pm$ 0.3	2.7 $\pm$ 1.4 $\pm$ 0.8
$\sum_i FF_i$	89.4 $\pm$ 0.3	115 $\pm$ 11 $\pm$ 8

Backup: Focus on $f_0(980)$ and $a_0(980)$ resonances

- BaBar considers only one of the two at the time
- Why?
- $f_0(980)$
  1. Charge: 0
  2. Spin: 0
  3. Mass: $980 MeV/c^2$
  4. Width: $10 - 100 MeV/c^2$
  5. Coupled channels: $\pi\pi, K\bar{K}$
- $a_0(980)$
  1. Charge: 0
  2. Spin: 0
  3. Mass: $980 MeV/c^2$
  4. Width: $50 - 100 MeV/c^2$
  5. Coupled channels: $\eta\pi, K\bar{K}$
- $A_{f_0} A_{a_0}$ gave one of the biggest interference fractions ($\sim 50\%$)
- Inlcusion of just one of the two: $f_0(980)$

Backup: BaBar LASS

- BaBar uses the LASS amplitude (from $K^-\pi^+ \to K^-\pi^+$ elastic scattering) for describing the D^0 decays into $K^\pm\pi^0$ S-wave states

$$A_{K\pi(S)}(s) = \frac{\sqrt{s}}{p} sin(\delta(s)) e^{i\delta(s)}$$

$$\delta(s) = cot^{-1}\left(\frac{1}{pa} + \frac{bp}{2}\right) + cot^{-1}\left(\frac{M_0^2 - s}{M_0 \Gamma_0 \frac{M_0}{\sqrt{s}} \frac{p}{p_0}}\right)$$

$$a = 1.95 \pm 0.09\, GeV^{-1}/c \quad b = 1.76 \pm 0.36\, GeV^{-1}/c$$

- The unitary nature of the latter eq provides a good description of the amplitude up to the $K\eta'$ threshold.
- The first term is a non-resonant contribution defined by a scattering length a and an effective range b, and the second term represents the $K_0^*(1430)$ resonance. The phase space factor $\sqrt{s}/p$ converts the scattering amplitude to the invariant amplitude.

Backup: Extra on BaBar LASS

- The unitary nature of the latter eq provides a good description of the amplitude up to the $K\eta'$ threshold
- $K_0^*(1430)$ Mass: $1425 \pm 50 MeV/c^2$, Width: $270 \pm 80 MeV$
  - $\rightarrow K\pi$: $BR \simeq 93\%$; $m(K\pi) \sim 629 MeV/c^2$
  - $\rightarrow K\eta'$: $BR \simeq 7\%$; $m(K\eta') \sim 1452 MeV/c^2$
- the description provided by the latter eq works up to the $K\eta'$ threshold
- for $\sqrt{s} \sim m(K\eta')$ the $K\eta'$ channel opens therefore an additional term should be added in the eq (sort of $K\pi \leftrightarrow K\eta'$ interference)?
  - like a coupled channels system (e.g. $f_0(980)$ in the KK S-Wave)

Backup: AmpGen LASS

- Brief description of the $K\pi$ S-wave based on the fits to scattering data. The LASS parametrization of the $K\pi$ S-wave is defined from fits to elastic $K\pi$ scattering data, which is approximately up to the $K\eta'$ threshold.

$$tg(\phi_{NR}) = \frac{2aq}{2 + arq^2} \quad tg(\phi_{BW}) = \frac{m\Gamma}{m^2 - s}$$
$$a = 2.07 \quad r = 3.32$$

- normally associated to the $K_0^*(1430)$ resonance.

$$\mathcal{A} = \frac{2a\sqrt{s}}{2 + arq^2 - 2iaq} + \frac{2 + arq^2 + 2iaq}{2 + arq^2 - 2iaq}\mathcal{A}_{\mathcal{BW}}(s) = A_{NR}(s) + A_{BW}^{'}(s)$$

- this expression resembles the sum of a BW with a slowly varying nonresonant component, the two parts are sometimes split apart with an additional production amplitude placed on one or the other

Backup: Comparison of BaBar and AmpGen LASS shapes

- BaBar

$$A_{K\pi(S)}(s) = \frac{\sqrt{s}}{p} sin(\delta(s)) e^{i\delta(s)}$$

$$\delta(s) = cot^{-1}\left(\frac{1}{pa} + \frac{bp}{2}\right) + cot^{-1}\left(\frac{M_0^2 - s}{M_0 \Gamma_0 \frac{M_0}{\sqrt{s}} \frac{p}{p_0}}\right)$$

- AmpGen

$$\mathcal{A} = \frac{2a\sqrt{s}}{2 + arq^2 - 2iaq} + \frac{2 + arq^2 + 2iaq}{2 + arq^2 - 2iaq} \times \frac{m\Gamma_0}{m^2 - s - im\Gamma} \frac{\sqrt{s}}{q}$$

- $\longrightarrow$ the two shapes provide quantitatively the same amplitude

Backup: BaBar Flatté

- The D^0 decay to a K^+K^- S-wave state is described by a coupled-channel BW amplitude for the $f_0(980)$ and $a_0(980)$ resonances, with their respective couplings to $\pi\pi$, $K\bar{K}$ and $\eta\pi$, $K\bar{K}$ final states.

$$A_{f_0}(s) = \frac{M_{D^0}^2}{M_0^2 - s - i(g_1^2\rho_{\pi\pi} + g_2^2\rho_{K\bar{K}})}$$

$$\rho = 2p/\sqrt{s}$$

$$M_0 = 965 \pm 10 MeV/c^2$$

$$g_1^2 = 165 \pm 18 MeV^2/c^4 \quad g_2^2/g_1^2 = 4.21 \pm 0.33$$

- the $f_0(980)$ values come from the BES collaboration
  - BES (Beijing Spectrometer) is an experiment at the Beijing Electron Positron Collider (BEPC)
- for the $a_0(980)$ the Crystal Barrel values are used [not reported]
  - Crystal Barrel was a detector at the Low Energy Antiproton Ring (LEAR) facility at CERN

Backup: AmpGen Flatté

- Lineshape to describe resonances with coupled channels such as $f_0(980)$ and $a_0(980)$.
- The lineshape was first described by S.M. Flatté [https://www.sciencedirect.com/science/article/pii/0370269376906547] and describes a single isolated resonance that couples to a pair of channels, which can have a large impact on the lineshape if the opening of one of the channels is near to the resonance mass.

$$A_{f_0}(s) = \frac{1}{m^2 - s - im\Gamma(s)}$$

$$\Gamma(s) = \frac{g_{\pi\pi}}{s}\lambda^{1/2}(s, m_\pi^2, m_\pi^2) + \frac{g_{KK}}{s}\lambda^{1/2}(s, m_K^2, m_K^2)$$

$$g_{\pi\pi} = 0.165 GeV/c^2 \quad \frac{g_{KK}}{g_{\pi\pi}} = 4.21$$

- this is for the $f_0(980)$ resonance.

Backup: More on the Flatté parametrization [1]

- Breit-Wigner:

$$\mathcal{A}(s) = \frac{1}{m_r^2 - s - i m_r \Gamma(s)}$$

- the RBW model is ideal when there is only one relevant decay channel (e.g. $\phi(1020) \to K^+K^-$)
- the other channels are much suppressed or not accessible kinematically; so only one channel contributes significantly
- the BW has a constant width o function of a single channel phase space
- What changes for the $f_0(980)$?
  - $f_0(980)$ can decay into $\pi\pi$ and $K\bar{K}$ $(K^+K^-, K^0\bar{K}^0)$
  - the mass of $f_0(980)$ is close to the $K\bar{K}$ threshold: $m(K^+K^-) \simeq 988 MeV/c^2$

Backup: More on the Flatté parametrization [2]

- Flatté model:

$$A_{f_0}(s) = \frac{1}{m^2 - s - i(g_1^2 \rho_{\pi\pi}(s) + g_2^2 \rho_{K\bar{K}}(s))}$$

$$\rho = \frac{2p}{\sqrt{s}} \quad p = \frac{\lambda^{1/2}(s, m_K^2, m_K^2)}{2\sqrt{s}} \quad \rho = \frac{\lambda^{1/2}(s, m_K^2, m_K^2)}{s}$$

- differently from the BW the total width depends on s and on which channels are open (kinematically allowed)
- there are coupling effects between the channels (interference)
  - being close to the $K\bar{K}$ threshold such effects and the dynamic effects at the threshold are important
- When s is under threshold for $K\bar{K}$ ($\sqrt{s} < 2m(K\bar{K})$), $\rho_{K\bar{K}}$ becomes immaginary (cause $\lambda^2 < 0$); for s getting close to the threshold this immaginary term varies rapidly.
- All this is treated unitarily with the Flatté model

Backup: Comparison of BaBar and AmpGen Flatté shapes

- BaBar

$$A_{f_0}(s) = \frac{M_{D^0}^2}{M_0^2 - s - i(g_1^2\rho_{\pi\pi} + g_2^2\rho_{K\bar{K}})} \quad \rho = 2p/\sqrt{s}$$

In the CM frame: $p = |\vec{p}| = \frac{\lambda^{1/2}(s,m_1^2,m_2^2)}{2\sqrt{s}}$, where λ is the Kallen function.

$\rho = 2p/\sqrt{s}$ in the formula becomes $\frac{\lambda^{1/2}}{s}$

$$A_{f_0}^{BaBar}(s) \rightarrow \frac{M_{D^0}^2}{M_0^2 - s - i(g_1^2\frac{\lambda_{\pi\pi}^{1/2}}{s} + g_2^2\frac{\lambda_{KK}^{1/2}}{s})}$$

- AmpGen

$$A_{f_0}^{AmpGen}(s) = \frac{1}{m^2 - s - im\left(g_{\pi\pi}\frac{\lambda^{1/2}(s,m_\pi^2,m_\pi^2)}{s} + g_{KK}\frac{\lambda^{1/2}(s,m_K^2,m_K^2)}{s}\right)}$$